Electronic Supplementary Material (ESI) for New Journal of Chemistry

Evidence of Ionic Liquid Crystal properties for a $DODA^+$ salt of the Keplerate $[Mo_{132}O_{372}(CH_3COO)_{30}(H_2O)_{72}]^{42-}$.

Sébastien Floquet,*[a] Emmanuel Terazzi,*[b] Akram Hijazi,[a,c] Laure Guénée,[b] Claude Piguet,[b] and Emmanuel Cadot[a]

[a] *Institut Lavoisier de Versailles, UMR 8180, University of Versailles Saint-Quentin, 45 av. des Etats-Unis, 78035 Versailles, France. Fax: +33 139254381; Tel: +33 139254379; E-mail: sebastien.floquet@chimie.uvsq.fr*

[b] *Department of Inorganic, Analytical and Applied Chemistry, University of Geneva, 30 quai E. Ansermet, CH-1211 Geneva 4, Switzerland. Fax: +41 223796830; Tel: +41 223796035; E-mail: emmanuel.terazzi@unige.ch*

[c] *Lebanese University, Doctoral School of Science and Technology, Research Platform for Environmental Science, Beirut, Lebanon.*

Supporting Information

(13 pages)

Experimental section

Physical methods

Infrared spectra were recorded on a Magna 550 Nicolet spectrophotometer, using KBr pellet.

Elemental analyses were performed by the service central d'analyses du CNRS, Vernaison, France and by the service d'analyses du CNRS, ICSN, Gif sur Yvette, France.

EDX measurements were performed on a JEOL JSM 5800LV apparatus.

Spectrophotometric studies were carried out on a Perkin Elmer Lambda 19 spectrophotometer at room temperature by using quartz cells of 1 mm path length.

TGA was performed with a Seiko TG/DTA 320 thermogravimetric balance (5°C min^{-1}, under N_2).

DSC traces were obtained with a Mettler Toledo DSC1 Star Systems differential scanning calorimeter from 3 to 5 mg samples (5°C min^{-1}, under N_2).

POM characterizations of the mesophases were performed with a Leitz Orthoplan Pol polarizing microscope with a Leitz LL 20×/0.40 polarizing objective and equipped with a Linkam THMS 600 variable temperature stage.

SA-XRD patterns were obtained with one experimental setup, the crude powder was filled in Lindemann capillaries of 0.8 mm diameter. Diffraction patterns were measured with a STOE transmission powder diffractometer system STADI P using a focused monochromatic Cu-$K_{\alpha 1}$ beam obtained from a curved Germanium monochromator (Johann-type) and collected on a curved image plate position-sensitive detector (IP-PSD). A calibration with silicon and copper laurate standards, for high and low angle domains, respectively, waspreliminarily performed. Sample capillaries were placed in the high-temperature attachment for measurements in the range of desired temperatures (from -30 up to 240°C) within 0.05 °C. Periodicities up to 50 Å could be measured. The exposure times were of 15 min.

Syntheses

The synthesis of the precursor $(NH_4)_{42}[Mo_{132}O_{372}(CH_3COO)_{30}(H_2O)_{72}]\cdot 300H_2O \cdot 10CH_3COONH_4$ was performed as described in literature (A. Müller, E. Krickemeyer, H. Bögge, M. Schmidtmann, F. Peters, *Angew. Chem. Int. Ed*., 1998, **37(24)**, 3359) and checked by routine methods (^{1}H NMR, FT-IR, UV-Visible spectroscopy). Solvents and Dimethyldioctadecylammonium chloride were purchased from from Acros or Aldrich Chemicals and used without further purification.

$(DODA)_{36}(NH_4)_6[Mo_{132}O_{372}(CH_3COO)_{30}(H_2O)_{72}]\cdot 75H_2O$, DODA-$Mo_{132}$,

4 g of the precursor $(NH_4)_{42}[Mo_{132}O_{372}(CH_3COO)_{30}(H_2O)_{72}]\cdot 300H_2O\cdot 10CH_3COONH_4$ (0.14 mmol)were solubilised in water (400 mL) to give a dark brown solution. To this solution was added a large excess of DODACl (15g, 25.6 mmol) solubilised in chloroform (400 mL) under vigorous stirring during 3 hours at room temperature. After almost complete extraction of Keplerate into the organic phase, the latter is separated by decantation and absolute ethanol (about 400 mL) are added, provoking the precipitation of the target compound as a black powder which was isolated by filtration, washed with ethanol and dried in air (m= 5.40 g, yield 90 %). FT-IR/cm^{-1}, (KBr pellet, Figures S1-S2): 2921(s), 2851(s), 1635(m), 1558(m), 1467(m), 981(s), 946(m), 861(s), 808(s), 732(s), 635(mw), 577(s), 471(mw). EDX: Absence of Cl, which excludes the presence of an excess of DODACl in the product. Elemental analysis calcd (%) for $(DODA)_{36}(NH_4)_6[Mo_{132}O_{372}(CH_3COO)_{30}(H_2O)_{72}].75H_2O$ (M = 42981.7 g mol^{-1}): C 39.90, H 7.71, N 1.37, Mo 29.46; found: C 39.85, H 7.51, N 1.26, Mo 29.28. TGA under N_2 or O_2: 6.0 to 6.5 % of weigth loss between 20°C and 220°C in agreement with the loss of the 75 hydration molecules and the 72 inner aquo ligands (theoritical weigth loss of 6.15 %). Decomposition above 260°C under N_2 (Figure S3) and above 220°C under O_2 (Figure S4). UV-visible spectrum ($CHCl_3$, 2.10^{-5} M, Figure S5): λ_{max} = 469 nm, ε_{max}= 336000 L.mol^{-1}.cm^{-1}.

Derivation of Equation 1 of the main text:

The volume of an hexagonal unit cell is given by Eq. I

$$V_{Hex} = \frac{a_{Hex}^2 (3)^{1/2} h}{2} \qquad \text{Eq.I}$$

The number of molecules per unit cell can be calculated using Eq. II

$$Z = \frac{dN_{AV} V_{Hex} 10^{-24}}{MM_C} \qquad \text{Eq.II}$$

Substitution of Eq II in Eq I leads to Eq. III

$$a_{Hex} = \left(\frac{2 \cdot Z \cdot MM_C}{h \cdot d \cdot N_{AV} \cdot 10^{-24} \cdot 3^{1/2}} \right)^{1/2} \qquad \text{Eq.III}$$

Table S1: Indexation at a Given Temperature for the Reflections Detected in the Liquid-Crystalline Phases by SA-XRD for Clusters **DODA-Mo$_{132}$**. Values are Given on Second Heating and Cooling.

T /°C	$d_{hkl\ (mes)}$ /Å	*I* /a.u.	*00l*	$d_{hkl\ (calc\ )}$ /Å	
240°C	27.27	VS(Sh)	001	26.96	*h* = 26.96 Å
	13.42	S(Sh)	002	13.48	a_{Hex}= 54.07 Å
Cooling	9.40[a]	S(Sh)			
	8.92	S(Sh)	003	8.99	
	4.50	W(Br)			
220°C	26.97	VS(Sh)	001	26.96	*h* = 26.90 Å
	13.30	S(Sh)	002	13.48	a_{Hex}= 54.13 Å
Cooling	9.37 [a]	S(Sh)			
	9.10	S(Sh)	003	8.99	
	4.50	W(Br)			
200°C	26.87	VS(Sh)	001	26.86	*h* = 26.86 Å
	13.28	S(Sh)	002	13.43	a_{Hex}= 54.17 Å
Cooling	9.32 [a]	S(Sh)			
	9.05	S(Sh)	003	8.95	
	4.50	W(Br)			
180°C	26.80	VS(Sh)	001	26.73	*h* = 26.73 Å
	13.19	S(Sh)	002	13.36	a_{Hex}= 54.31 Å
Cooling	9.30 [a]	S(Sh)			
	9.00	S(Sh)	003	8.91	
	4.50	W(Br)			
160°C	26.50	VS(Sh)	001	26.50	*h* = 26.50 Å
	13.25	S(Sh)	002	13.25	a_{Hex}= 54.54 Å
Cooling	9.24 [a]	S(Sh)			
	4.50	W(Br)			
140°C	26.48	VS(Sh)	001	26.34	*h* = 26.34 Å
	13.10	S(Sh)	002	13.17	a_{Hex}= 54.71 Å
Cooling	9.22 [a]	S(Sh)			
	4.50	W(Br)			
120°C	26.40	VS(Sh)	001	26.26	*h* = 26.26 Å
	13.06	S(Sh)	002	13.13	a_{Hex}= 54.79 Å
Cooling	9.21 [a]	S(Sh)			
	4.50	W(Br)			
100°C	26.27	VS(Sh)	001	26.11	*h* = 26.11 Å
	12.97	S(Sh)	002	13.05	a_{Hex}= 54.95 Å
Cooling	9.15 [a]	S(Sh)			
	4.50	W(Br)			

80°C	26.07	VS(Sh)	001	25.93	h = 25.93 Å
	12.89	S(Sh)	002	12.96	a_{Hex}= 55.14 Å
Cooling	9.12 [a]	S(Sh)			
	4.50	W(Br)			
60°C	25.97	VS(Sh)	001	25.73	h = 25.73 Å
	12.74	S(Sh)	002	12.86	a_{Hex}= 55.35 Å
Cooling	9.12 [a]	S(Sh)			
	4.50	W(Br)			
40°C	25.42	VS(Sh)	001	25.21	h = 25.21 Å
	12.50	S(Sh)	002	12.61	a_{Hex}= 55.92 Å
Cooling	9.09 [a]	S(Sh)			
	4.50	W(Br)			
20°C	25.09	VS(Sh)	001	24.84	h = 24.84 Å
	12.29	S(Sh)	002	12.42	a_{Hex}= 56.33 Å
Cooling	9.00 [a]	S(Sh)			
	4.50	W(Br)			
0°C	24.63	VS(Sh)	001	24.51	h = 24.51 Å
	12.19	S(Sh)	002	12.25	a_{Hex}= 56.71 Å
Cooling	8.91 [a]	S(Sh)			
	4.50	W(Br)			
-10°C	24.66	VS(Sh)	001	24.45	h = 24.45 Å
	12.12	S(Sh)	002	12.23	a_{Hex}= 56.78 Å
Cooling	8.93 [a]	S(Sh)			
	4.50	W(Br)			
-20°C	24.38	VS(Sh)	001	24.35	h = 24.35 Å
	12.16	S(Sh)	002	12.18	a_{Hex}= 56.90 Å
Cooling	8.92 [a]	S(Sh)			
	4.50	W(Br)			
-30°C	24.52	VS(Sh)	001	24.32	h = 24.32 Å
	12.06	S(Sh)	002	12.16	a_{Hex}= 56.93 Å
Cooling	8.93 [a]	S(Sh)			
	4.50	W(Br)			
-20°C	24.56	VS(Sh)	001	24.34	h = 24.34 Å
	12.06	S(Sh)	002	12.17	a_{Hex}= 56.91 Å
Heating	8.92 [a]	S(Sh)			
	4.50	W(Sh)			
-10°C	24.62	VS(Sh)	001	24.37	h = 24.37 Å
	12.06	S(Sh)	002	12.19	a_{Hex}= 56.87 Å
Heating	8.93 [a]	S(Sh)			
	4.50	W(Br)			

0°C	24.66	VS(Sh)	001	24.48	h = 24.48 Å
	12.15	S(Sh)	002	12.15	a_{Hex}= 56.75 Å
Heating	8.94 [a]	S(Sh)			
	4.50	W(Br)			
20°C	25.02	VS(Sh)	001	24.78	h = 24.78 Å
	12.27	S(Sh)	002	12.27	a_{Hex}= 56.40 Å
Heating	9.00 [a]	S(Sh)			
	4.50	W(Br)			
40°C	25.38	VS(Sh)	001	25.13	h = 25.13 Å
	12.44	S(Sh)	002	12.57	a_{Hex}= 56.01 Å
Heating	9.06 [a]	S(Sh)			
	4.50	W(Br)			
60°C	25.89	VS(Sh)	001	25.75	h = 25.75 Å
	12.80	S(Sh)	002	12.87	a_{Hex}= 55.33 Å
Heating	9.10 [a]	S(Sh)			
	4.00	W(Br)			
80°C	26.17	VS(Sh)	001	25.97	h = 25.97 Å
	12.88	S(Sh)	002	12.98	a_{Hex}= 55.09 Å
Heating	9.12 [a]	S(Sh)			
	4.50	W(Br)			
100°C	26.29	VS(Sh)	001	26.12	h = 26.12 Å
	12.97	S(Sh)	002	13.06	a_{Hex}= 54.94 Å
Heating	9.13 [a]	S(Sh)			
	4.50	W(Br)			
120°C	26.42	VS(Sh)	001	26.23	h = 26.23 Å
	13.02	S(Sh)	002	13.12	a_{Hex}= 54.82 Å
Heating	9.19 [a]	S(Sh)			
	4.50	W(Br)			
140°C	26.46	VS(Sh)	001	26.30	h = 26.30 Å
	13.07	S(Sh)	002	13.15	a_{Hex}= 54.75 Å
Heating	9.21 [a]	S(Sh)			
	4.50	W(Br)			
160°C	26.55	VS(Sh)	001	26.43	h = 26.43 Å
	13.15	S(Sh)	002	13.21	a_{Hex}= 54.61 Å
Heating	9.25 [a]	S(Sh)			
	4.50	W(Br)			
180°C	26.71	VS(Sh)	001	26.55	h = 26.55 Å
	13.19	S(Sh)	002	13.27	a_{Hex}= 54.49 Å
Heating	9.27 [a]	S(Sh)			
	4.50	W(Br)			

200°C	26.95	VS(Sh)	001	26.79	h = 26.79 Å
	13.31	S(Sh)	002	13.39	a_{Hex}= 54.25 Å
Heating	9.34 [a]	S(Sh)			
	4.50	W(Br)			
220°C	27.15	VS(Sh)	001	26.93	h = 26.93 Å
	13.35	S(Sh)	002	13.46	a_{Hex}= 54.10 Å
Heating	9.37 [a]	S(Sh)			
	4.50	W(Br)			
240°C	27.27	VS(Sh)	001	27.05	h = 27.05 Å
	13.41	S(Sh)	002	13.52	a_{Hex}= 53.98 Å
Heating	9.41 [a]	S(Sh)			
	4.50	W(Br)			

[a] Even if we do not have irrefutable argument to support this hypothesis, the presence of this additional reflection is probably due to short contact distances between the surfaces of metallic cores of the clusters since the h periodicity is slightly shorter than the cluster core diameter. $d_{hkl\ (mes)}$ and $d_{hkl\ (calc)}$ are the measured and calculated diffraction spacing ; h is the lattice parameter of the smectic phase ; I corresponds to the intensity of the reflections (VS : very strong, S : strong, W : weak ; br and sh stand for broad and sharp) ; h and $d_{hkl\ (calc\ )}$ are respectively calculated according the formula : $h = 1/3\ (d_{001(exp)} + 2d_{002\ (exp)} + 3d_{003\ (exp)})$ and $d_{hkl\ (calc)} = h/l$; a_{Hex} is the local hexagonal organization within the layers calculated with eq 1.

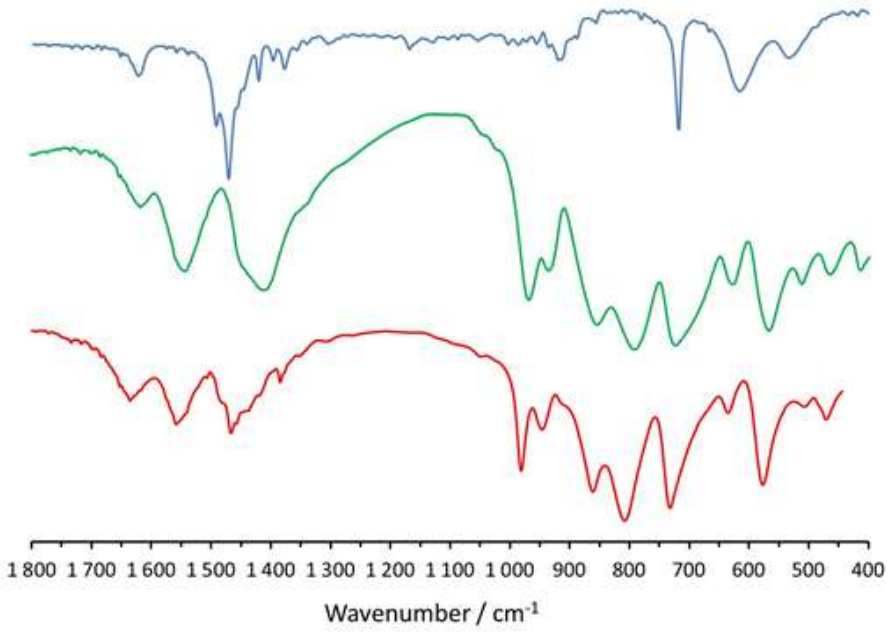

Figure S1: FT-IR spectra of DODACl (blue), $(NH_4)_{42}[Mo_{132}O_{372}(CH_3COO)_{30}(H_2O)_{72}]\cdot 300H_2O\cdot 10CH_3COONH_4$ (green) and **DODA-Mo$_{132}$** (red) in the 1800-400 cm^{-1} range.

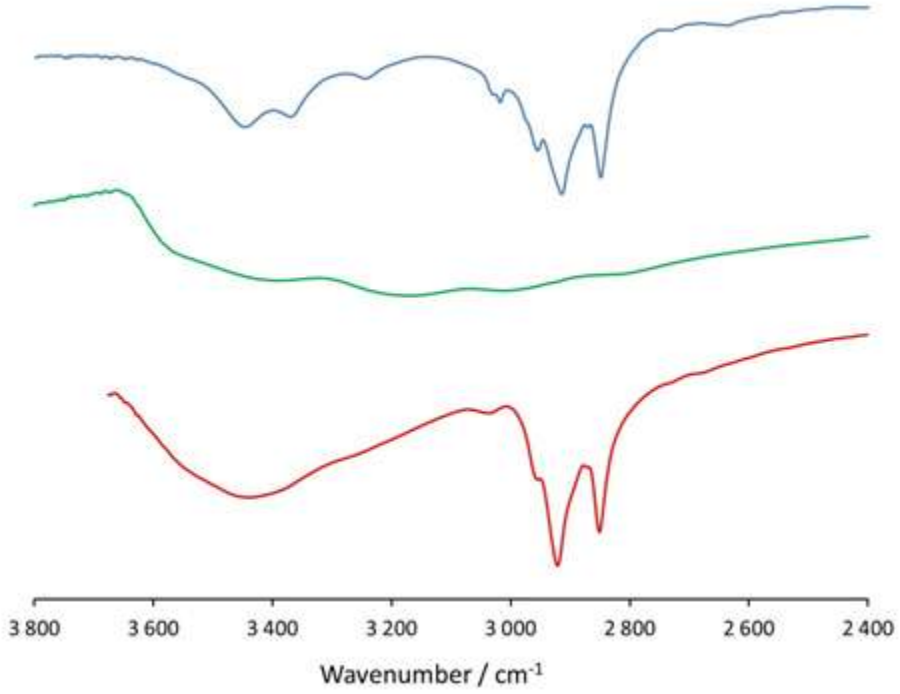

Figure S2: FT-IR spectra of DODACl (blue), $(NH_4)_{42}[Mo_{132}O_{372}(CH_3COO)_{30}(H_2O)_{72}]\cdot 300H_2O\cdot 10CH_3COONH_4$ (green) and **DODA-Mo$_{132}$** (red) in the 3800-2400 cm^{-1} range.

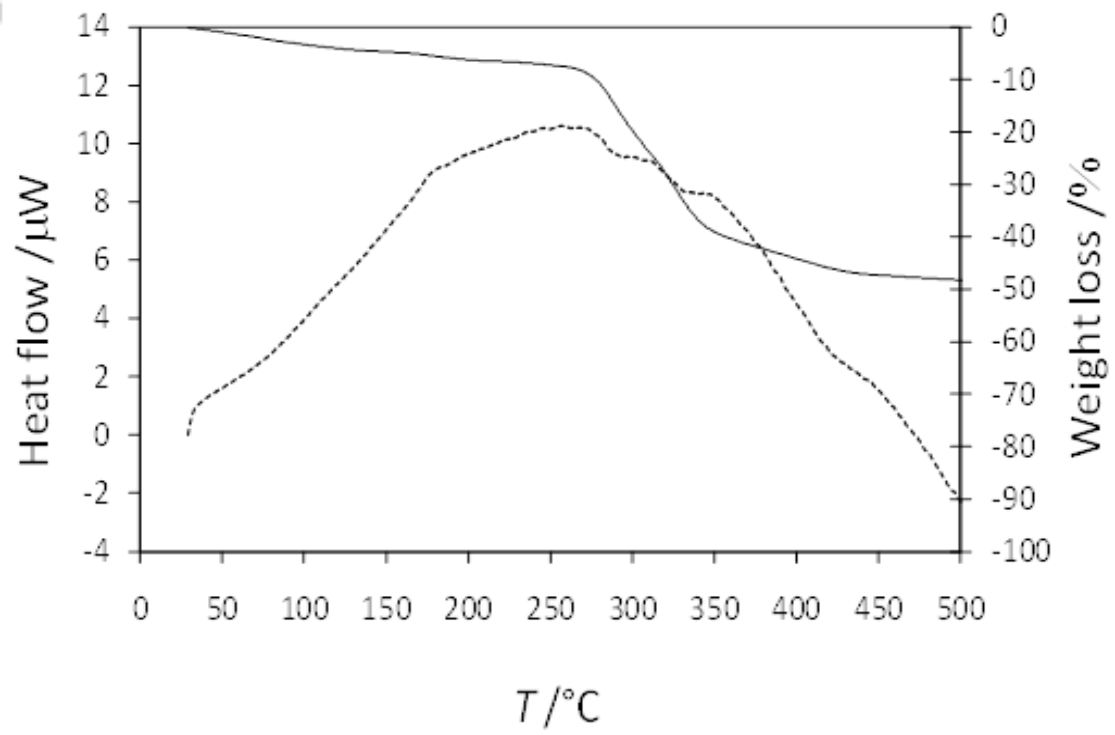

Figure S3: TGA Trace of **DODA-Mo$_{132}$** under N_2 (5°C min^{-1})

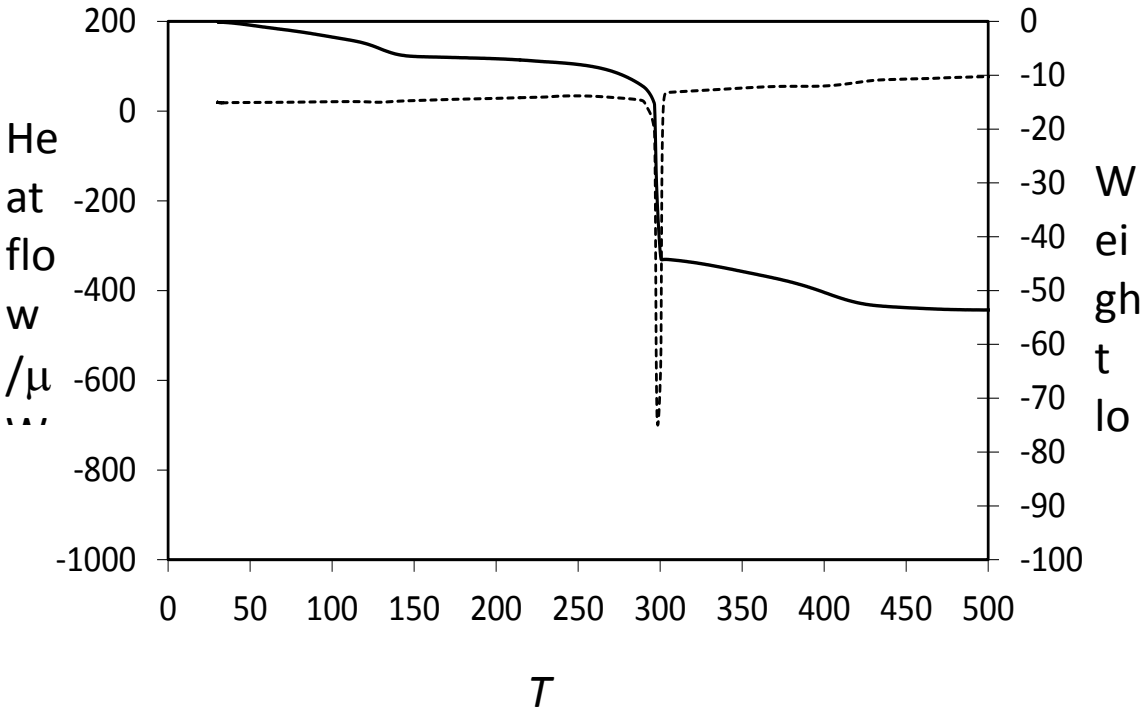

Figure S4: TGA Trace of **DODA-Mo$_{132}$** under O_2 (5°C min^{-1})

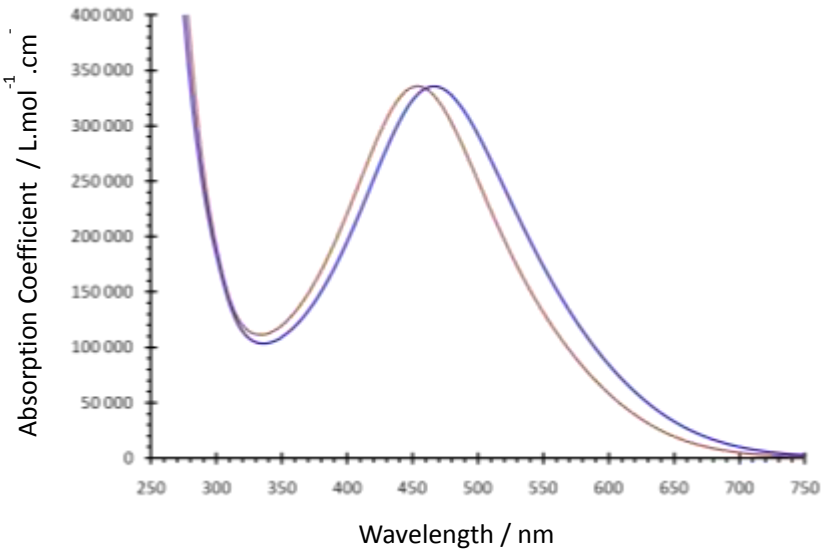

Figure S5: Electronic spectrum of a 2.10^{-5} M solution of **DODA-Mo$_{132}$** in $CHCl_3$ (blue) compared to the electronic spectrum recorded for a 2.10^{-5} M solution of $(NH_4)_{42}[Mo_{132}O_{372}(CH_3COO)_{30}(H_2O)_{72}]\cdot 300H_2O\cdot 10CH_3COONH_4$ in water (red). The comparison of both spectra confirms that the integrity of the keplerate architecture is maintained between these both clusters.

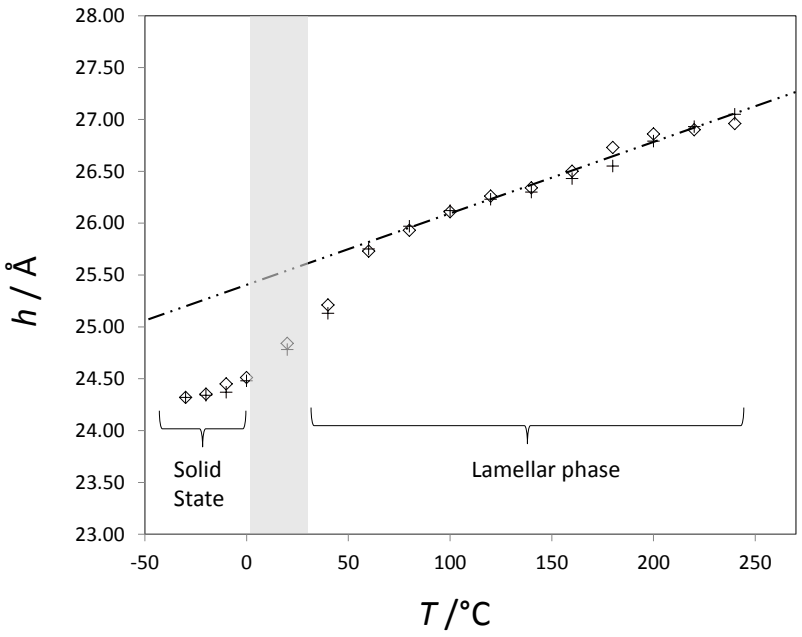

Figure S6: Evolution of the lattice parameter *h* for **DODA-Mo$_{132}$** as function of the temperature. The grey rectangle is the width of the phase transition. The "+" are the data recorded on heating and the "◊" are the data recorded during the cooling.

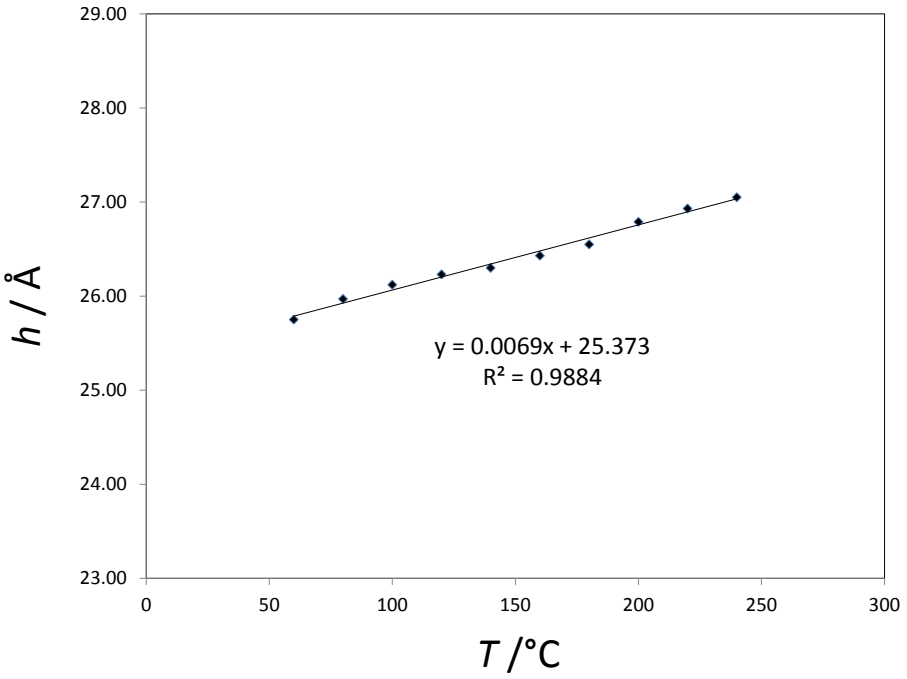

Figure S7: linear fit of the lattice parameter *h* of **DODA-Mo$_{132}$** on heating in the 60 to 260°C temperature range.

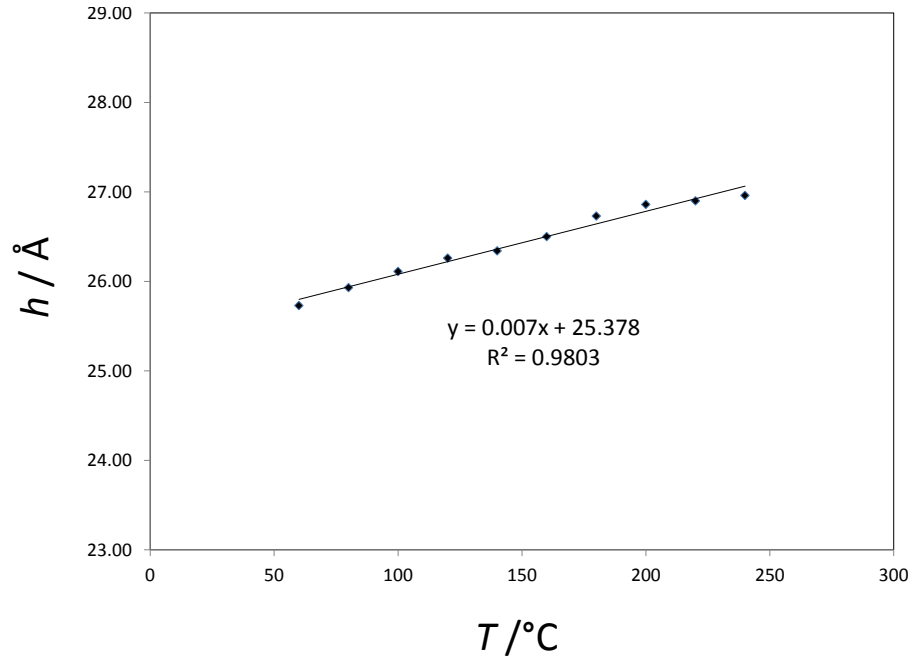

Figure S8: linear fit of the lattice parameter *h* of **DODA-Mo$_{132}$** on cooling in the 60 to 260°C temperature range.

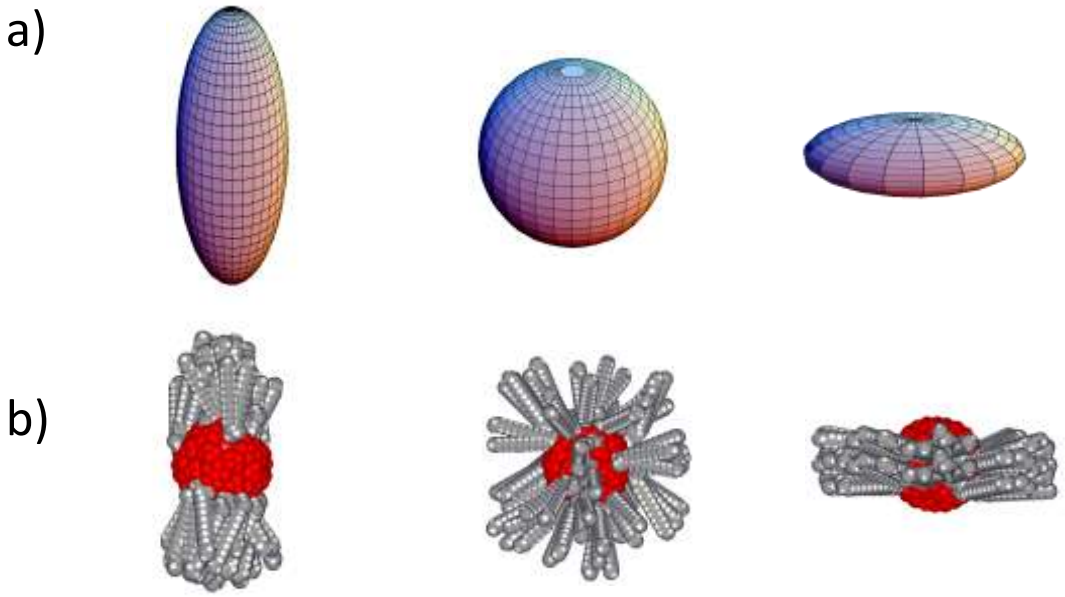

Figure S9: (a) prolate ellipsoid (left), sphere (center), oblate ellipsoid (right); (b) corresponding prolate cluster (left), spherical cluster (center) and oblate cluster (right).